Journal of Geoscience and Environment Protection, 2025, 13(4), 113-140
https://www.scirp.org/journal/gep
ISSN Online: 2327-4344
ISSN Print: 2327-4336

Hydrochemical Dispersion and Geospatial Correlation for Source Identification, Transport, and Fate of Aerial Petro-Pollutants in the Niger Delta, Nigeria

Nurudeen Ahmed Onomhoale[1*], Luqman Jibril Yunusa[2], Samson Senbore[3], Moses Dolapo Apata[4#], Percy Ojogbo[5], Emmanuel Samson Itiveh[6]

[1]Department of Civil Engineering, Faculty of Engineering, Universiti Putra Malaysia (UPM), Serdang, Malaysia
[2]Institute of Mining, National University of Science and Technology MISiS, Moscow, Russia
[3]Department of Geology, Faculty of Natural and Agricultural Sciences, University of Pretoria, Gauteng, South Africa
[4]School of Management, University of Bradford, Bradford, UK
[5]Department of Petroleum and Gas Engineering, Delta State University of Science and Technology, Ozoro, Nigeria
[6]Geoscience and Environment, Petrous Eco Geosolutions, Port Harcourt, Nigeria
Email: *nurudeenonomhoale@gmail.com

How to cite this paper: Onomhoale, N. A., Yunusa, L. J., Senbore, S., Apata, M. D., Ojogbo, P., & Itiveh, E. S. (2025). Hydrochemical Dispersion and Geospatial Correlation for Source Identification, Transport, and Fate of Aerial Petro-Pollutants in the Niger Delta, Nigeria. *Journal of Geoscience and Environment Protection, 13,* 113-140.
https://doi.org/10.4236/gep.2025.134007

Received: February 24, 2025
Accepted: April 11, 2025
Published: April 14, 2025

Abstract

The Niger Delta region of Nigeria is heavily impacted by petroleum exploration, refining activities, and industrial emissions, contributing to widespread aerial petro-pollutant contamination. This study investigates the hydrochemical dispersion and geospatial correlation of atmospheric petroleum hydrocarbons (TPH) deposited through rainfall within selected locations in Rivers State, Nigeria. Thirty-four rainwater samples were collected from seven distinct sub-regional study locations: Obigbo, Komkom, Obiama, Okoloma, Egberu, Umu Agbai, and Obete. Hydrochemical analyses were conducted using gas chromatography-flame ionization detection (GC-FID) to quantify total petroleum hydrocarbons (TPH), with detailed compositional profiling of aliphatic hydrocarbons (C8 - C40) and polycyclic aromatic hydrocarbons (PAHs). The dispersion analysis employed Hexbin density mapping, Contour visualization, and spatial interpolation techniques to delineate pollution hotspots, revealing significant contamination gradients across the study region. The correlation matrix assessed interrelationships between hydrocarbon fractions and geographic positioning, identifying strong positive correlations ($r > 0.9$) between TPH and total aliphatic hydrocarbons (TAH), suggesting transportation and industrial emissions as primary sources. PAHs exhibited localized concentration spikes,

*Corresponding author.
#"School of Management, University of Bradford, Bradford, UK" is Moses Dolapo Apata's previous work address.

particularly near gas flaring zones and commercial hubs, implicating fossil fuel combustion, industrial activities, and long-range pollutant transport as dominant contamination mechanisms. Geospatial analysis indicates higher hydrocarbon deposition in the Western and Northern regions, with Obigbo and Okoloma experiencing the most significant contamination. The study highlights rainfall as a key vector for atmospheric petrochemical deposition, with implications for water quality, ecosystem health, and human exposure risks. These findings emphasize the need for stricter environmental monitoring, regulatory enforcement of industrial emissions, and strategic efforts to mitigate hydrocarbon pollution in petroleum-producing regions.

Keywords

Hydrochemical Analysis, Spatio-Density Analysis, Total Petroleum Hydrocarbons (TPH) Contamination, Aerial Deposition, Correlation Matrix Analysis, Python Geospatial Data Visualization

1. Introduction

Water is a fundamental resource for sustaining life, supporting agriculture, domestic use, industrial applications, and ecosystem health (Ahmed et al., 2024b). Its quality is influenced by natural processes and anthropogenic activities, with contamination posing significant risks to environmental sustainability and human well-being (Alao et al., 2024). In petroleum-rich regions such as the Niger Delta, hydrocarbon pollution remains a critical concern due to extensive oil exploration, refining, and associated industrial activities (George et al., 2023). The release of petrochemical pollutants into the environment, mainly through aerial deposition, contributes to the degradation of water resources, impacting both human health and ecological systems (Chinedu & Chukwuemeka, 2018).

Petro-pollutants, especially airborne contaminants from gas flaring, fossil fuel combustion, and crude oil volatilization, are transported through the atmosphere and deposited via precipitation, affecting terrestrial and aquatic ecosystems (Bebeteidoh et al., 2020). Gas flaring, a common industrial practice in the Niger Delta, releases particulate matter, including soot laden with total petroleum hydrocarbons (TPH), into the atmosphere (Ahmed et al., 2024d). These pollutants interact with atmospheric moisture, leading to the deposition of hydrocarbon-laden rainwater, which subsequently infiltrates surface and groundwater systems, altering their physicochemical and geochemical properties (Okorhi-Damisa et al., 2020). Rainfall, a vector for atmospheric pollutants, facilitates the transport and accumulation of hydrocarbons in water bodies, soil matrices, and vegetation. These pollutants pose significant environmental and public health risks, given the toxicity and persistence of petroleum hydrocarbons, including aliphatic hydrocarbons and polycyclic aromatic hydrocarbons (PAHs) (Ahmed et al., 2024b).

The hydrochemical dispersion of targeted aerial petro-pollutants offers an approach to understanding the distribution and interaction of hydrocarbon contam-

inants within affected regions (Schwarzenbach et al., 2005). This analytical framework integrates three critical dimensions: hydrology, chemistry, and spatial dynamics, each of which plays a pivotal role in determining the fate and transport of pollutants (Koch & Schneider, 2019). The hydrological aspect focuses on the role of water as a medium for pollutant dispersion, examining pathways such as atmospheric precipitation, surface runoff, and groundwater flow (Baker & Sillanpää, 2017). The chemical component explores the physicochemical characteristics of pollutants, including their composition (Ahmed et al., 2024a), degradation processes, and reactivity, with particular emphasis on the toxicity and persistence of petroleum hydrocarbons (Manisalidis et al., 2020). The dispersion dimension addresses spatial variation, proportional distributions, and density mapping, which govern pollutants' deposition, movement, and accumulation across different environmental compartments (Moore et al., 2023). Understanding these interconnected processes is essential for assessing the contamination dynamics of petro-pollutants and their broader implications for environmental health and water quality management (UNEP, 2021).

The multivariate correlation using a matrix is a statistical tool for evaluating the interrelationships among hydrochemical parameters, pollutant variables and geographic positioning, offering insights into contamination trends and source identification (Fawole et al., 2016). By analyzing the degree of association between key parameters, this study aims to elucidate the extent to which various pollutants co-occur and influence water quality (AICHAW, 2010). Strong correlations between certain hydrocarbon fractions and specific water quality indicators may suggest common contamination pathways through atmospheric deposition, surface runoff, or subsurface infiltration (Liu & Wang, 2019). Furthermore, the correlation matrix can aid in distinguishing between natural geochemical influences and anthropogenic hydrocarbon inputs, providing a robust framework for pollution source apportionment and risk assessment (Baker & Cormier, 2017). Through this approach, this research contributes to a more precise understanding of the systemic interactions governing hydrocarbon pollution in the Niger Delta, enhancing the effectiveness of environmental management strategies and policies (Eneji & Ogban, 2020).

The hydrochemical dynamics and interactions of petro-pollutants influence their spatial distribution, transport mechanisms, and ecological impact. Soot-derived hydrocarbons, particularly PAHs, are of significant concern due to their carcinogenic potential and ability to bioaccumulate in ecosystems (Zhou et al., 2020). In the Niger Delta, the complex hydro-topographical and climatic conditions modulate the dispersion and deposition patterns of these pollutants, necessitating a systematic approach to monitoring their environmental impact (Samuel et al., 2022; Ahmed et al., 2024c). Given the increasing prevalence of hydrocarbon contamination in the region, there is a critical need for data-driven analyses to evaluate pollution hotspots and assess the vulnerability of affected water bodies (Ojelede & Kafadar, 2023). Identifying these areas is essential for mitigating contamination risks, as prolonged exposure to hydrocarbon pollutants can lead to

severe environmental degradation and public health concerns (Eneji & Ogban, 2020). The integration of hydrochemical assessments, spatial mapping, and correlation analysis will provide a more comprehensive understanding of pollution dynamics, supporting targeted intervention measures to enhance water quality and environmental resilience in the Niger Delta (Ojelede & Kafadar, 2023).

This study aims to conduct a hydrochemical dispersion of targeted aerial petropollutants in atmospheric water systems within the primary oil-producing locations of the South-East senatorial district region of Rivers State, Niger Delta, Nigeria. It seeks to examine the geospatial distribution, concentration gradients, and correlation matrix of TPH contaminants, emphasizing the interrelationships between atmospheric deposition, hydrological pathways, and environmental vulnerability. By integrating hydrochemical assessments with geospatial mapping and correlation, this research provides critical insights into pollution dynamics, water quality degradation, and the broader environmental risks associated with petroleum-derived atmospheric pollutants. The findings of this study are essential for sustainable water resource management, environmental monitoring, and regulatory policy development. Furthermore, the study contributes valuable empirical data to inform researchers, environmental regulators, and government agencies in designing effective mitigation strategies to protect public health and promote ecological resilience in petroleum-producing communities.

2. Methodology

2.1. Data Acquisition and Analysis

2.1.1. Field Sampling

The study involved the collection of thirty-four rainwater samples collected directly during precipitation using a purpose-built rainwater harvesting system, ensuring minimal external contamination. Before collection, all sampling bottles were pre-sterilized, and the water was subsequently transferred into 1.5-litre plastic water sampling containers for preservation and further analysis. The fieldwork was structured by grouping the seven study sub-regions into five distinct locations: Obigbo, Komkom-Obiama, Okoloma, Egberu, and Umu Agbai-Obete (**Table 1**). Settlements, markets, schools, hospitals, and petroleum facilities were mapped within these sub-regional locations, and samples were systematically collected. Systematic random sampling was employed to achieve an even spatial distribution across the study area, with precise coordinates and sampling station recording, ensuring a representative analysis (Daniel, 2003; Teixeira & Nearing, 2019). The geo-referencing of all sampling points and study area location mapping was conducted using the Garmin eTrex 32x, a rugged Handheld GPS device, ensuring precise spatial documentation of sample collection sites (Ahmed et al., 2024b). To maintain sample integrity, all collected samples were immediately transferred to plastic containers, preserved in ice-packed coolers, and promptly transported to the laboratory. This stringent sample handling protocol prevented contamination and degradation for accurate hydrochemical analysis.

Table 1. Locations and sample stations.

ID	Locations	Stations	Latitude (N)	Longitude (E)
OYB 1	Obigbo	Primary Health Centre	4.8763330	7.1135890
OYB 2		Timber Market	4.8731770	7.1176030
OYB 3		Main Market	4.8782510	7.1457740
OYB 4		Atata Market	4.8837610	7.1305650
OYB 5		Umuebele Market	4.8988195	7.1364424
OYB 6		CSS Umudinor	4.8814128	7.1267495
OYB 7		CSS Umuakpahu	4.8821758	7.1266840
OYB 8		Oasis Orphanage	4.8922960	7.1083230
OYB 9		Shell Location Facility	4.8922022	7.1226464
OYB 10	Komkom-Obiama	Konko Market	4.8563490	7.1822390
OYB 11		CSS Komkom	4.8577900	7.1752860
OYB 12		Lekuma Township	4.8514200	7.1935470
OYB 13		Komkom Township	4.8578428	7.1593367
OYB 14		Obiama Township	4.8419240	7.1939940
OYB 15	Okoloma	Okoloma Market	4.8498900	7.2458800
OYB 16		Umuosi Market	4.8632450	7.2978980
OYB 17		Ayama Township	4.8527000	7.2641900
OYB 18		Afam Township	4.8512500	7.2375100
OYB 19		Obumku Township	4.8591700	7.2817800
OYB 20		Okoloma Gas Plant	4.8445051	7.2535040
OYB 21		Afam Power Plant	4.8481780	7.2568750
OYB 22	Egberu	Ndoki Health Centre	4.8521190	7.3183670
OYB 23		Ndoki Market	4.8490560	7.3269170
OYB 24		CSS Ndoki	4.8498670	7.3244060
OYB 25		Afam-Uku Township	4.8166700	7.3166700
OYB 26		Ndoki Township	4.8098212	7.2801760
OYB 27		Afam-Nta Township	4.8069030	7.3423580
OYB 28	Umu Agbai-Obete	Ban-Lori Market	4.8063200	7.4320200
OYB 29		Obete Township	4.8109700	7.4872400
OYB 30		Umu Agbai Township	4.8534300	7.3773800
OYB 31		Okpontu Township	4.8349300	7.4588400
OYB 32		Azuagu Township	4.8475990	7.3931630
OYB 33		Marihun Township	4.8577550	7.3721830
OYB 34		Azumini Township	4.8432820	7.4504320

2.1.2. Hydrochemical Analysis

The hydrochemical analysis involved the evaluation of total petroleum hydrocar-

bon (TPH) content in water samples, which was conducted to determine the concentrations of both petroleum aliphatic hydrocarbons and petroleum aromatic hydrocarbons. Gas Chromatography (GC) analysis was employed using an Agilent 7820A gas chromatograph equipped with a flame ionization detector (FID) and an HP-5 fused silica capillary column (30 m × 0.32 mm ID × 0.25 μm film thickness). The purified sample extracts were analyzed with helium as the carrier gas, set at a flow rate of 1.75 mL/min and an average velocity of 29.47 cm/sec. The injection was performed in splitless mode, where 1 μL of the sample extract was introduced at an injection temperature of 300˚C. The column temperature was programmed to start at 40˚C for 1 minute, then ramped at 7˚C/min until reaching a final temperature of 320˚C. The detector temperature was maintained at 300˚C throughout the process, following the established methodology of Kim, Hong, and Won (2013) and Inyang, Aliyu, and Oyewale (2018).

To ensure analytical accuracy, GC calibration was performed using petroleum hydrocarbon calibration standards ranging from 0.05 - 20 μg/mL, with n-hexane as the diluent. Calibration curves were generated using Agilent Chemstation chromatography software, and average response factors for each analyte were calculated. The calibration results demonstrated high linearity, with correlation coefficients (R^2) ranging from 0.9846 to 0.9919, ensuring reliable quantification of hydrocarbons. Unresolved peaks were quantified using the response factor nC-15, following the approach outlined by Luan and Szelewski (2008). The determination of TPH concentrations involved baseline integration and peak sum slicing, covering the hydrocarbon range from nC-9 to nC-36 and the unresolved complex mixture (UCM). Further hydrocarbon profiling was conducted by calculating the ratios of low molecular weight n-alkanes to high molecular weight n-alkanes and unresolved n-alkanes to resolved n-alkanes, as Inyang et al. (2018) described. This analytical protocol ensured precise quantification and characterization of petroleum hydrocarbons, providing critical insights into contamination levels in the sampled water bodies.

2.1.3. Dispersion and Correlation Analysis

The dispersion analysis of targeted aerial petro-pollutants was conducted to characterize the proportional distribution and density mapping of total petroleum hydrocarbons (TPH) across the study area. This approach integrates density representation, spatial analysis and contour overlay techniques to assess the extent and intensity of hydrocarbon contamination in atmospheric water systems (Mohamed et al., 2024). The analysis employed Contour and Hexbin plots to visualize pollutant distribution and highlight key contamination zones (Hengl & Gould, 2002), depicting contamination density variations and effectively revealing pollution hotspots and concentration gradients across the locations and sample stations (Antai et al., 2018). This approach adopts triangular or hexagonal grids, where each triangle or hexagon represents the average TPH concentration within that localized region.

To further investigate the interrelationships among hydrochemical variables, a

multivariate correlation matrix was developed to identify significant correlations between key hydrochemical parameters, including total petroleum hydrocarbons (TPH) fractions and the geographical positioning of sample stations (Hodge & Hoque, 2011). By analyzing correlation coefficients, the study aimed to determine how much hydrocarbon pollutants co-occur with other environmental variables, offering insights into contamination trends and possible pollution sources (Dale & Boulton, 2019). Strong correlations between hydrocarbon fractions and particular hydrochemical indicators suggested potential common contamination pathways (Dale & Boulton, 2019). Also, the correlation matrix helped differentiate influences from anthropogenic hydrocarbon inputs, enhancing pollution source identification and risk assessment (Hodge & Hoque, 2011). The analysis and visualization were done using Python-based geospatial and scientific visualization libraries, incorporating Matplotlib, SciPy, and Seaborn (Müller & Meyer, 2021).

Integrating dispersion and correlation analyses strengthened the study's ability to characterize pollutant behaviour, map contamination intensity, and identify underlying hydrochemical relationships within the study region (Sadiq & Al-Sharif, 2020). By leveraging multiple techniques and overlap plots for pollutant distribution and correlation matrix for statistical assessment, this approach provided a comprehensive and multidimensional evaluation of hydrocarbon pollution in the Niger Delta. These findings contribute valuable empirical data for environmental monitoring, pollution control strategies, and water quality management, supporting efforts to mitigate contamination risks and promote sustainable water resource management in petroleum-producing regions (Sadiq & Al-Sharif, 2020).

2.2. Study Location and Stations

The study area falls within the primary oil-producing locations of the South-East senatorial district region of River State and is situated around the Oyigbo, Eleme, Tai, and Khana Local Government Areas (LGAs), however, principally located in the Oyigbo LGA, Niger Delta, Nigeria. The key reference location is situated approximately 30 kilometres Northeast of Port Harcourt. It lies within the geographic coordinates of latitude 4.9000˚N to 4.7667˚N and longitude 7.2500˚W to 7.4167˚W (**Figure 1**). The Asa and Ndoki predominantly inhabited the area, contributing to its rich cultural and ethnic diversity (Opu-Ogulaya, 1973). The region plays a strategic role in the socio-economic and political landscape of Rivers State, forming a key part of the Niger Delta region (Obenade et al., 2020).

Population trends indicate substantial growth, rising from 40,407 in 1975 to 125,666 in 2015, reflecting increased urbanization and economic activities in the area (NBS, 2006). The demographic expansion is largely driven by the availability of dry land and favorable terrain, which supports settlement and industrialization (Samuel et al., 2022). The region experiences a tropical wet climate characterized by prolonged rainy seasons and short dry seasons. The dry season spans November to February, with December being the driest month. Heavy precipitation occurs in September, averaging 370 mm, while the annual mean rainfall is approxi-

mately 2500 mm, mostly concentrated between May and October (Onwuka et al., 2021). Temperature variations remain minimal, ranging between 25˚C and 28˚C throughout the year, while relative humidity fluctuates from 80% during the rainy season to around 40% in the dry season (Ahmed et al., 2024b). The vegetation consists mainly of tropical rainforest along river systems, interspersed with secondary bushlands resulting from farming and fallowing activities (Onwuka et al., 2021).

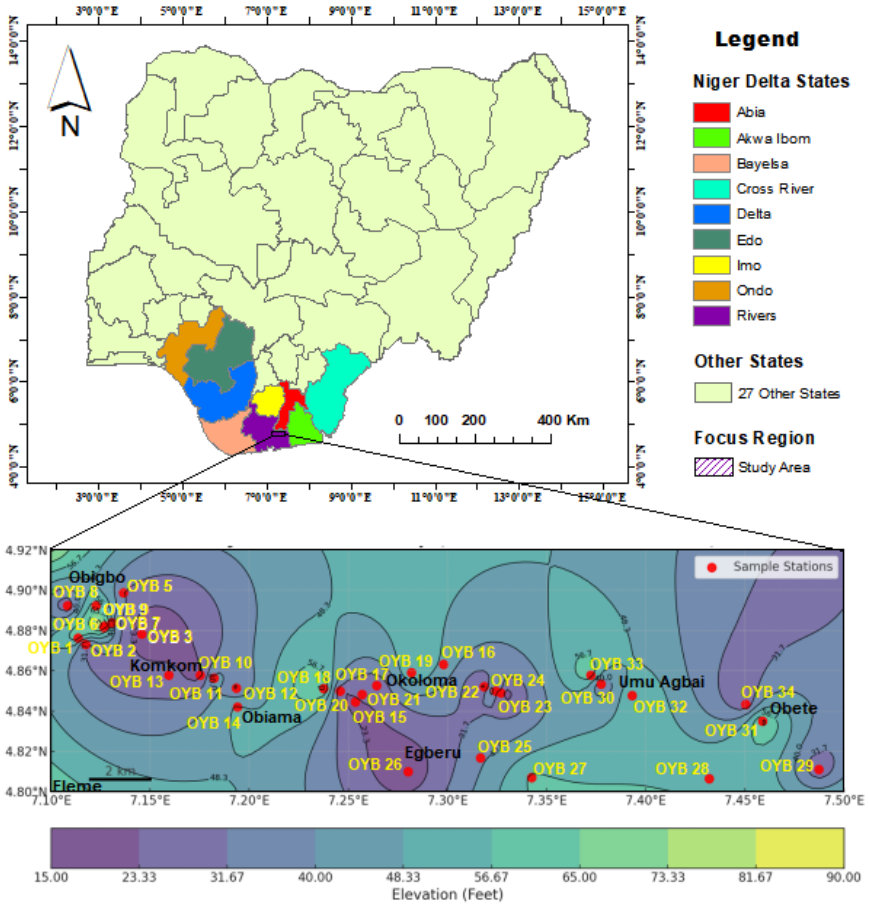

Figure 1. Map showing Nigeria, niger delta, rivers state, study locations, and sample stations. (Source: Digitized by Author)

The target study location is a key oil-producing region and a major industrial hub, hosting several multinational petroleum firms (Enotoriuwa et al., 2016). The discovery of crude oil has significantly transformed the local economy, with major petroleum infrastructure such as the Afam Power Station, Shell Okoloma Gas Plant, and Nigerian Gas Plant Plc serving as primary revenue generators (Ahmed et al., 2024c). However, these facilities also contribute to environmental challenges, including hydrocarbon pollution and land degradation, necessitating sustainable management strategies (Omokpariola et al., 2022). The rapid urban expansion has been fueled by affordable housing relative to Port Harcourt, leading to increased migration and traffic congestion as workers commute daily to the city

(Samuel et al., 2022). As an industrial and commercial centre, the Oyigbo region continues to experience significant environmental pressures, highlighting the need for comprehensive pollution assessment and management strategies to mitigate the impact of petroleum-related activities on water and soil quality.

3. Results and Discussions

To facilitate the petro-pollutants characterization in the study locations, the total petroleum hydrocarbon (TPH) was analyzed using polycyclic aromatic hydrocarbons (PAH) and total aliphatic hydrocarbons (TAH) fractions. The PAH include sixteen components which are Naphthalene, Methylnapthylene, Acenaptylene, Acenaphthlene, Fluorene, Phenanthrene, Anthracene, Pyrene, Chrysene, Fluoranthene, Benzo [a] Anthracene, Benzo [b] Fluoranthene, Benzo [k] Fluoranthene, Benzo [a] Pyrene, Indenol [1, 2, 3-cd] pyrene, and Dibenzo [a, h] Anthracene, with their concentrations assessed across various study locations. The TAH fraction, which spanned C8 to C40, was further categorized into three distinct groups: Lighter Aliphatic Hydrocarbons (C8 - C16), Medium Aliphatic Hydrocarbons (C17 - C24), including Pristane and Phytane, and Heavy Aliphatic Hydrocarbons (C25 - C40). This classification allowed for a structured approach to analyzing hydrocarbon distribution and compositional variations, ensuring a meaningful evaluation of environmental impacts (Omokpariola et al., 2022).

3.1. Hydrochemical Dispersion Analysis

3.1.1. Hexbin and Contour Analysis for Obigbo

The hexbin and contour overlay plots provide a spatial and geometric representation of TPH concentration levels at different sampling stations within the Obigbo location (**Figures 2(a)-(d)**). The Contour Plot uses color gradients to depict concentration variations, while the Hexbin highlights measured sample densities. High PAH concentrations (**Figure 2(a)**), indicated by red/maroon zones, were observed at stations such as OYB 5, OYB 9, and OYB 4, corresponding to Umuebele Market, Shell Facility, and Atata Market, which are linked to petroleum spills, vehicular emissions, and industrial discharges (Ahmed et al., 2024a). Low PAH concentrations, represented by blue zones, were recorded at OYB 3 (Main Market), where reduced contamination suggests lower hydrocarbon inputs or natural attenuation (Li & Wong, 2018). The combined plot refines observations by characterizing pollution hotspots with dense hexagonal bins. These findings highlight the influence of industrial and commercial activities in PAH distribution, with vehicular emissions and petroleum residues as likely contributors (Mason & Brubaker, 2019; Nadim & Hossain, 2021).

The plot for C8 to C16 TAHs (**Figure 2(b)**) indicates contamination trends across the area. Higher concentrations were detected at OYB 4 (Atata Market), OYB 9 (Shell Facility), and OYB 7 & OYB 6 (CSS Umuakpahu & CSS Umudinor), which are areas associated with fuel residues, vehicular emissions, and industrial activities (Nadim & Hossain, 2021). Lower concentrations were present at OYB 3

(Main Market) and OYB 1 (Health Center), likely due to natural dispersion or minimal hydrocarbon sources. The volatility of C8 to C16 hydrocarbons suggests that while these compounds degrade faster, their presence in residential and commercial zones poses air quality and water contamination risks (Cohen & Coyle, 2019).

The C17 to C24 fraction (**Figure 2(c)**) represents semi-volatile hydrocarbons with longer environmental persistence. The plot highlights elevated levels at OYB 4 (Atata Market), OYB 9 (Shell Facility), and OYB 7 & OYB 6 (CSS Umuakpahu & CSS Umudinor), suggesting persistent contamination from industrial and vehicular sources. Lower concentrations were observed at OYB 3 (Main Market), OYB 1 (Health Center), and OYB 2 (Timber Market), implying reduced hydrocarbon input (Hwang & Park, 2021).

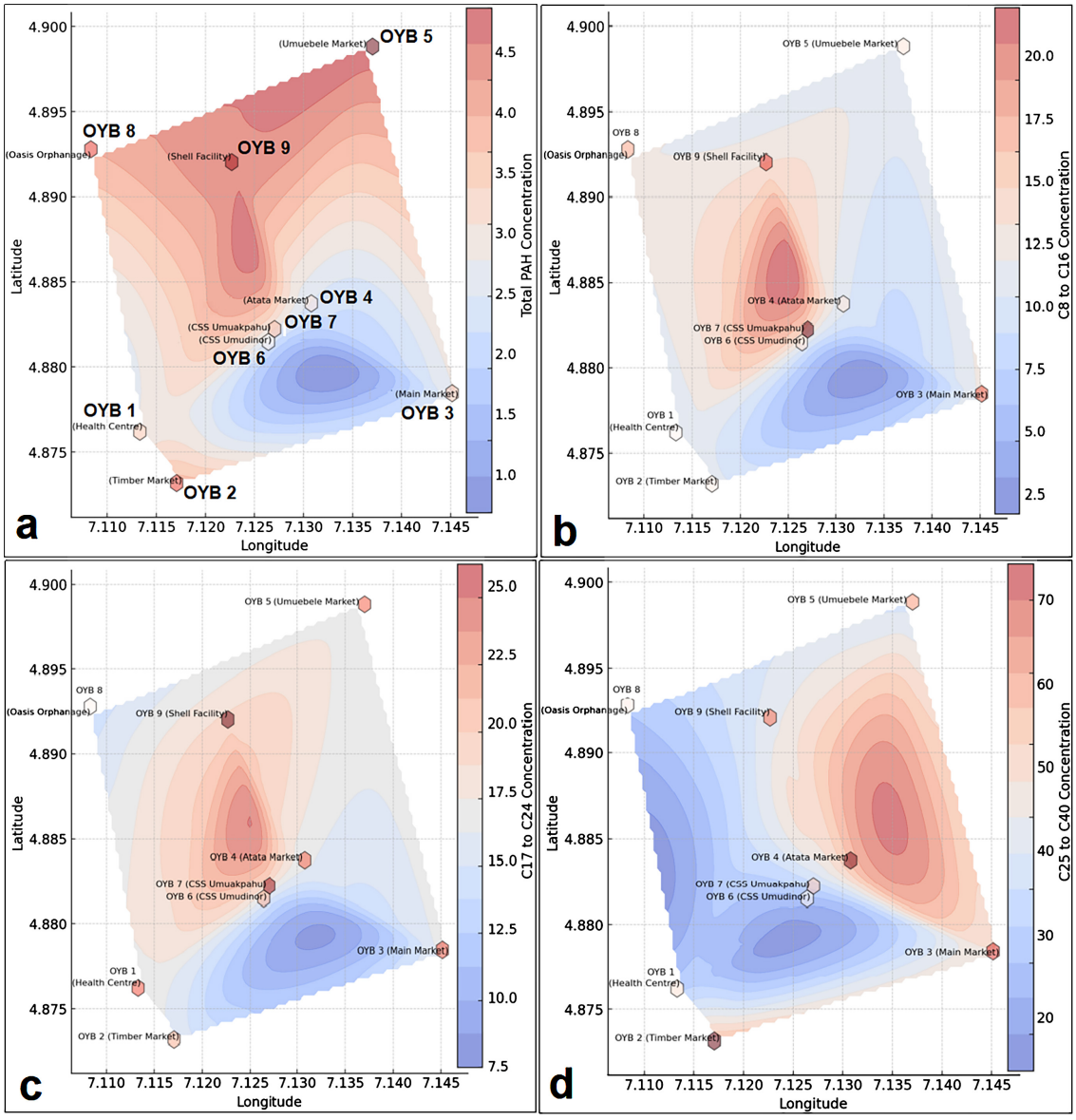

Figure 2. Dispersion for Obigbo. a) Total PAH, b) C8 to C16, c) C17 to C24, and d) C25 to C40 aliphatics.

Given their lower degradation rates, C17 to C24 contribute to long-term soil and water pollution, emphasizing needs for sustained monitoring. The heavy C25 to C40 is highly persistent, with a strong affinity for water and soil, leading to long-term contamination risks (Nadim & Hossain, 2021). **Figure 2(d)** reveals high levels at OYB 4 (Atata Market), OYB 9 (Shell Facility), and OYB 5 (Umuebele Market), confirming the influence of petroleum residues and industrial emissions. Lower levels were found at OYB 3 (Main Market), OYB 1 (Health Center), and OYB 2 (Timber Market), implying reduced pollutants. The Hexbin Overlay enhances visualization by representing each station contamination value, highlighting localized pollution severity. Due to their low volatility, C25 to C40 hydrocarbons persist in industrial locations, increasing ecological and human health risks (George et al., 2023).

3.1.2. Hexbin and Contour Analysis for Komkom-Obiama

The Total PAH across the Komkom-Obiama location, as shown in **Figure 3(a)**, was represented using a contour and hexbin overlay visualization, which revealed distinct spatial variations in contamination levels. High PAH concentrations were recorded at OYB 10 (Konko Market) and OYB 12 (Lekuma Township), indicating strong influences from petroleum spills, vehicular emissions, and industrial activities (Cohen & Coyle, 2019). Lower PAH concentrations were observed at OYB 13 (Komkom Township), OYB 14 (Obiama Township), and OYB 11 (CSS Komkom), suggesting reduced contamination or possible natural attenuation (Li & Wong, 2018). The contour interpolation further highlighted an increasing concentration gradient in high-traffic and industrial zones, emphasizing the necessity for remediation and pollution control strategies (Liu & Liu, 2020). The C8 - C16 fraction of TAH, depicted in **Figure 3(b)**, exhibited elevated concentrations at OYB 13 (Komkom Township), likely due to petroleum-related activities, fuel emissions, and industrial processes (Nadim & Hossain, 2021). Conversely, lower concentrations were recorded at OYB 12 (Lekuma Township) and OYB 14 (Obiama Township), suggesting lower contamination exposure. The high volatility of the C8 - C16 fraction may explain its wider dispersion, requiring a monitoring approach that considers airborne transport and infiltration into surface waters (Cohen & Coyle, 2019).

The C17 - C24 fraction, including Pristane and Phytane, exhibited more persistent environmental presence, as shown in **Figure 3(c)**. High concentrations were recorded at OYB 13 (Komkom Township), OYB 11 (CSS Komkom), and OYB 10 (Konko Market), indicating long-term retention and reduced degradation of these hydrocarbons (Häggblom & Bossert, 2021). Lower concentrations were noted at OYB 12 (Lekuma Township) and OYB 14 (Obiama Township), reinforcing the role of dispersion in these areas (Siciliano & Enkiri, 2019). The semi-volatile nature of this fraction highlights its potential for soil adsorption and secondary contamination, which calls for further sediment and water quality assessments. The C25 - C40 fraction, which consists of heavier hydrocarbons, demonstrated localized contamination patterns with limited mobility, as illustrated in **Figure 3(d)**.

Strong concentration zones were identified at OYB 13 (Komkom Township), OYB 11 (CSS Komkom), and OYB 10 (Konko Market), where petroleum residues and industrial discharge appear to be dominant contamination sources.

Lower concentrations were observed at OYB 12 (Lekuma Township) and OYB 14 (Obiama Township), indicating less contamination or enhanced degradation mechanisms in these zones (Ghosh & Sinha, 2020). Due to their high persistence and strong soil-binding capacity, C25 - C40 hydrocarbons pose long-term contamination risks, necessitating targeted remediation efforts focused on hydrocarbon sequestration in soil and sediments (Fang & Zhao, 2021). The systematic classification and visualization of TPH fractions at the Komkom-Obiama Axis provided critical insights into contamination distribution and potential environmental risks. The observed higher PAH and TAH (C8 - C40) concentrations in industrial and commercial areas underline the influence of petroleum activities,

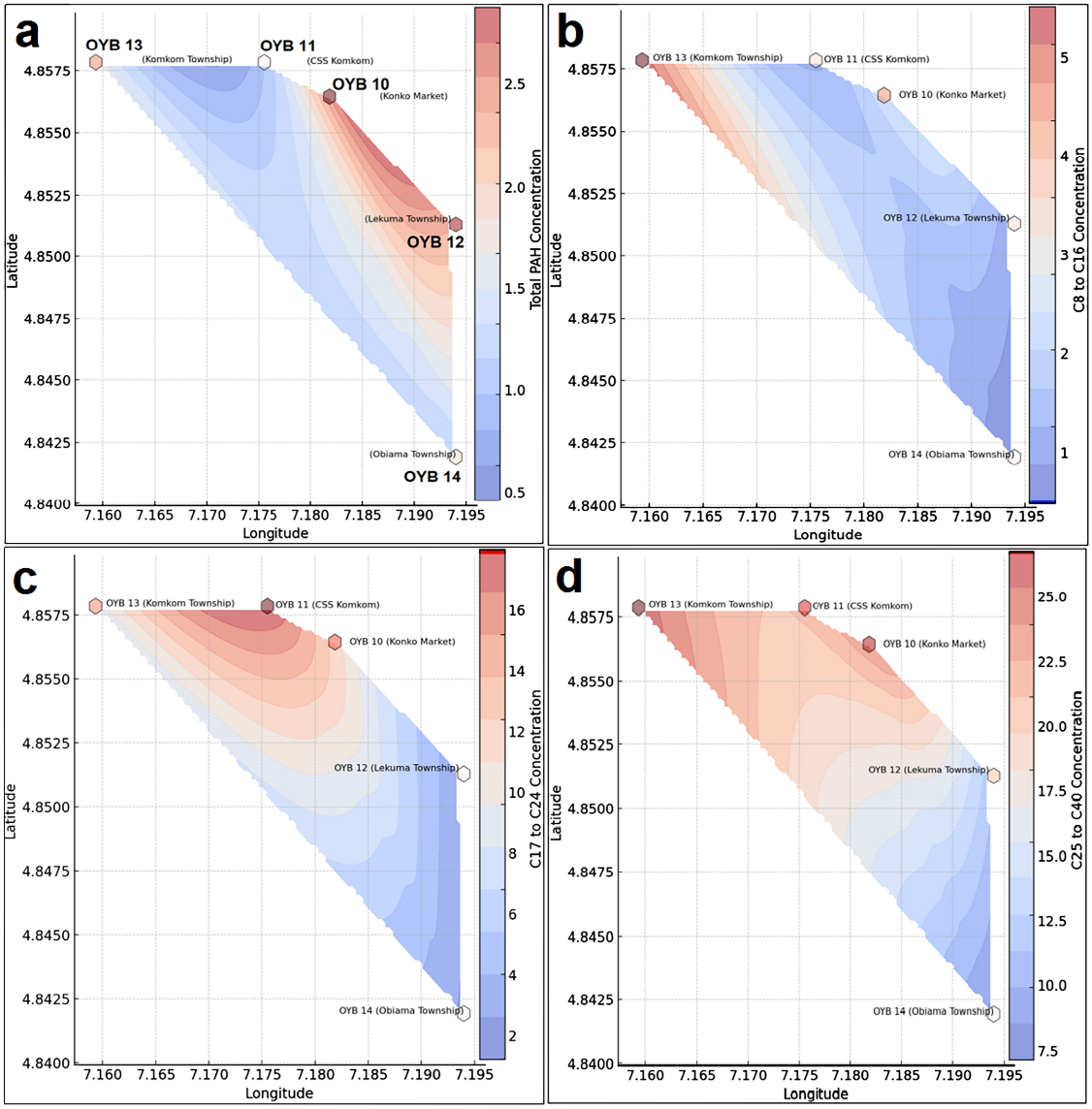

Figure 3. Dispersion for Komkom-Obiama. a) Total PAH, b) C8 to C16, c) C17 to C24, and d) C25 to C40 aliphatics.

fuel combustion, and industrial emissions (Zhang & Zhang, 2019; Cohen & Coyle, 2019). Meanwhile, lower contamination levels near residential areas and community service locations may indicate dispersion effects, natural attenuation, or limited hydrocarbon inputs (Häggblom & Bossert, 2021). The study revealed that lighter hydrocarbons (C8 - C16) exhibit wider dispersion, whereas heavier fractions (C25 - C40) demonstrate localized persistence, necessitating tailored mitigation strategies.

3.1.3. Hexbin and Contour Analysis for Okoloma

The Total PAH concentration across the Okoloma location (**Figure 4(a)**) revealed distinct spatial variations in contamination levels. High PAH concentrations were recorded at OYB 17 (Ayama Township) and OYB 20 (Okoloma Gas Plant), indicating strong influences from petroleum spills, gas flaring, and industrial emissions.

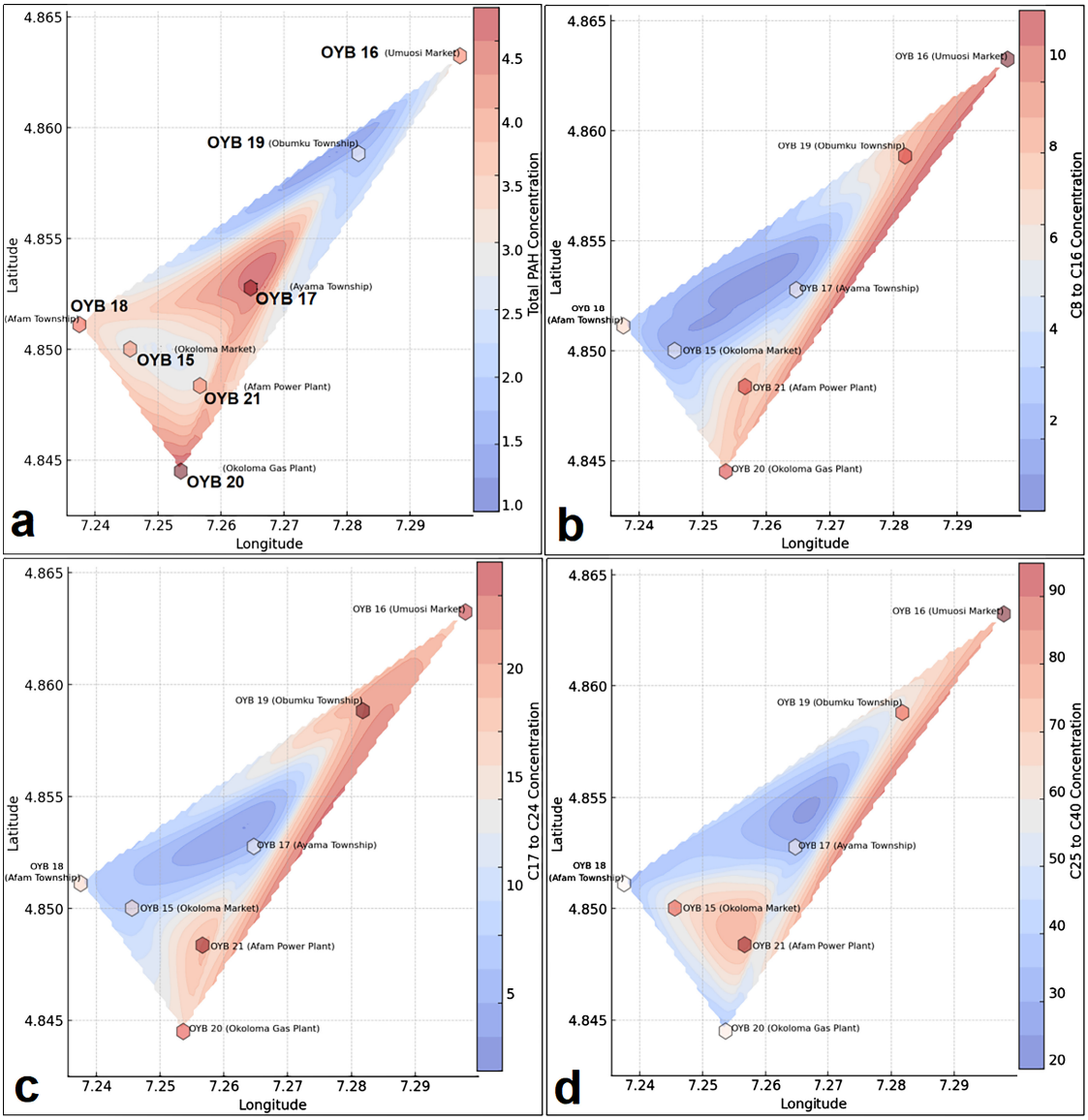

Figure 4. Dispersion for Okoloma. a) Total PAH, b) C8 to C16, c) C17 to C24, and d) C25 to C40 aliphatics.

Lower PAH concentrations were observed at OYB 19 (Obumku Township) and OYB 16 (Umuosi Market), suggesting reduced contamination or possible natural attenuation. The contour interpolation further highlighted an increasing concentration gradient in high-traffic and industrial zones, emphasizing the necessity for pollution control strategies. The C8 - C16 fraction of TAH, depicted in **Figure 4(b)**, exhibited elevated concentrations at OYB 16 (Umuosi Market), OYB 20 (Okoloma Gas Plant), and OYB 21 (Afam Power Plant) due to petroleum-related activities, fuel emissions, and industrial processes (Rapaport & Guers, 2019). Conversely, lower concentrations were recorded at OYB 15 (Okoloma Market) and OYB 17 (Ayama Township), suggesting lower contamination exposure. The high volatility of the C8 - C16 fraction may explain its wider dispersion, requiring a monitoring approach considering airborne transport and infiltration into surface waters (Rapaport & Guers, 2019).

The C17 - C24 fraction, including Pristane and Phytane, exhibited more persistent environmental presence, as shown in **Figure 4(c)**. High concentrations were recorded at OYB 16 (Umuosi Market), OYB 19 (Obumku Township), OYB 20 (Okoloma Gas Plant), and OYB 21 (Afam Power Plant), indicating long-term retention and reduced degradation of these hydrocarbons (Lima & Mata, 2021). Lower concentrations were noted at OYB 15 (Okoloma Market) and OYB 17 (Ayama Township), reinforcing the role of natural attenuation and dispersion in these areas. The semi-volatile nature of this fraction highlights its potential for soil adsorption and secondary contamination, which calls for further sediment and water quality assessments (Chen & Zhang, 2020).

The C25 - C40 fraction, which consists of heavier hydrocarbons, demonstrated localized contamination patterns with limited mobility (**Figure 4(d)**). Strong concentration zones were identified at OYB 16 (Umuosi Market), OYB 19 (Obumku Township), and OYB 21 (Afam Power Plant), where petroleum residues and industrial discharge appear to be dominant contamination sources. Lower concentrations were observed at OYB 17 (Ayama Township) and OYB 20 (Okoloma Gas Plant), indicating less contamination in these zones (Chen & Zhang, 2020). Due to their high persistence and strong soil-binding capacity, C25 - C40 hydrocarbons pose long-term contamination risks, necessitating targeted efforts focused on hydrocarbon sequestration in soil and sediments (Chen & Zhang, 2020).

3.1.4. Hexbin and Contour Analysis for Egberu

The Total PAH (**Figure 5(a)**) revealed distinct spatial variations in contamination levels across the Egberu. High PAH concentrations were observed at OYB 23 (Ndoki Market) and OYB 24 (CSS Ndoki), indicating strong influences from commercial activities, petroleum contamination, and vehicular emissions (González & Aroca, 2021). Lower PAH was detected at OYB 25 (Afam-Uku Township) and OYB 26 (Ndoki Township), suggesting lower contamination exposure or effective natural attenuation mechanisms (Crump & Smith, 2020). The colour interpretation of the contour and hexbin overlay revealed that red/maroon regions correspond to high PAH concentrations, while blue regions indicate lower PAH con-

tamination. The neutral/white areas represent moderate contamination levels, forming transitional zones between highly contaminated and less impacted areas. The hexbin overlay further reinforces these findings, as hexagonal bins with darker red intensities confirm measured high PAH levels in key industrial and commercial zones (Hwang & Kim, 2020; Frolova & Guo, 2020).

The C8 - C16 fraction of TAH (**Figure 5(b)**) exhibited spatial variability across the Egberu location, with elevated contamination in commercial and industrial locations. Higher C8 - C16 concentrations were recorded at OYB 22 (Ndoki Health Centre), OYB 23 (Ndoki Market), and OYB 24 (CSS Ndoki), likely due to petroleum-related contamination, vehicular emissions, and commercial activities (Rapaport & Guers, 2019). In contrast, lower concentrations were noted at OYB 25 (Afam-Uku Township), OYB 26 (Ndoki Township), and OYB 27 (Afam-Nta

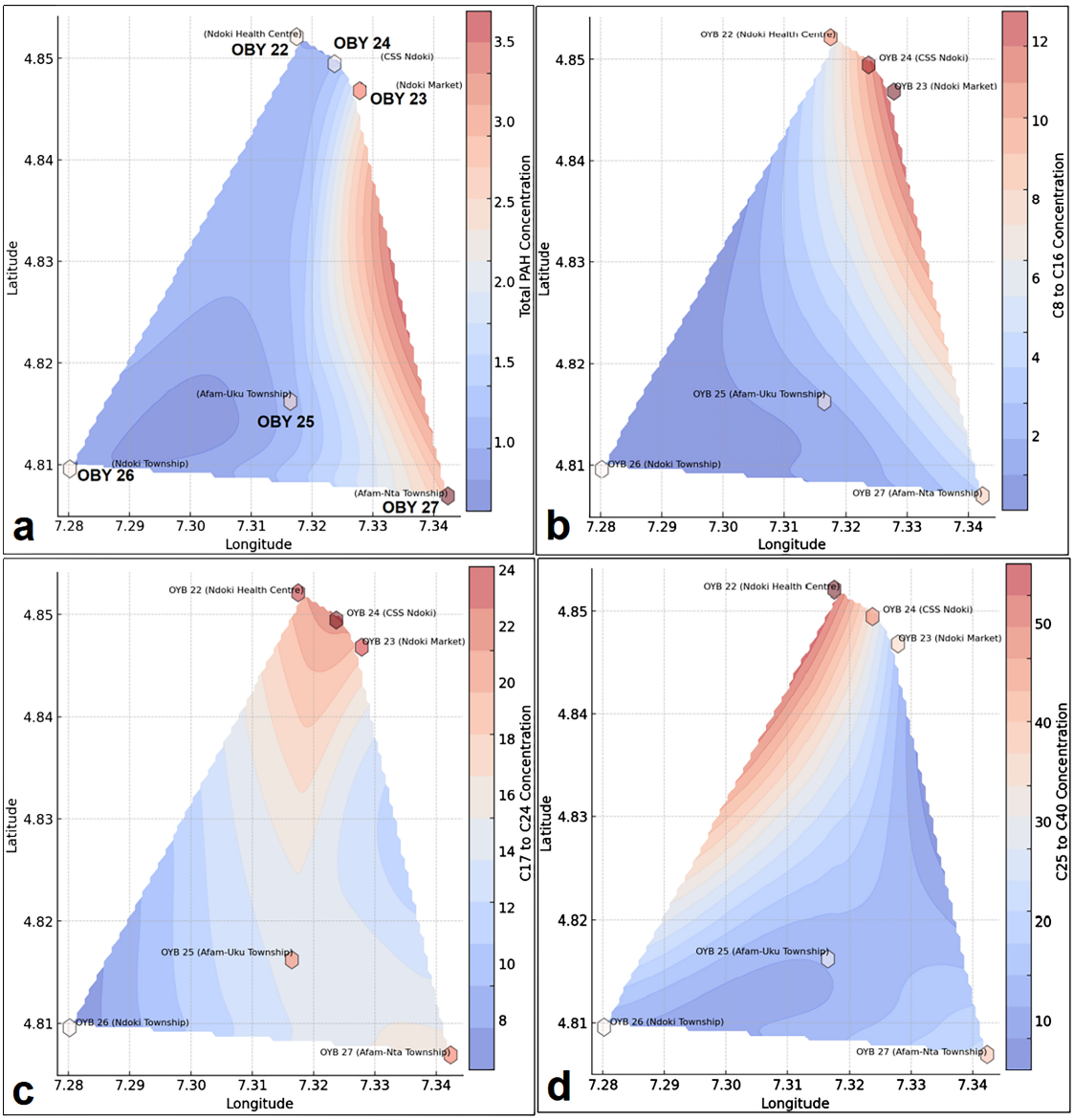

Figure 5. Dispersion for Egberu. a) Total PAH, b) C8 to C16, c) C17 to C24, and d) C25 to C40 aliphatics.

Township), implying natural dispersion or reduced contamination input. The C8 - C16 fraction is more volatile and degrades faster than heavier hydrocarbons; however, its presence in high-traffic areas raises concerns about airborne and soil contamination risks (Rapaport & Guers, 2019).

The C17 - C24 fraction of TAH, depicted in **Figure 5(c)**, exhibited a more persistent environmental presence across the study area. Higher concentrations were recorded at OYB 22 (Ndoki Health Centre), OYB 23 (Ndoki Market), and OYB 24 (CSS Ndoki), indicating long-term retention and reduced degradation of these hydrocarbons (Kumar & Singh, 2018; Lima & Mata, 2021). Meanwhile, lower concentrations were observed at OYB 25 (Afam-Uku Township), OYB 26 (Ndoki Township), and OYB 27 (Afam-Nta Township), reinforcing the role of natural attenuation and dispersion in these areas (Chen & Zhang, 2020). The C25 - C40 fraction of TAH, as illustrated in **Figure 5(d)**, demonstrated localized contamination patterns with limited mobility across the study area. Strong concentration zones were identified at OYB 22 (Ndoki Health Centre), OYB 23 (Ndoki Market), and OYB 24 (CSS Ndoki), where petroleum residues and industrial discharges appeared to be the dominant contamination sources. Lower concentrations were observed at OYB 25 (Afam-Uku Township), OYB 26 (Ndoki Township), and OYB 27 (Afam-Nta Township), suggesting reduced contamination exposure (Crump & Smith, 2020).

3.1.5. Hexbin and Contour Analysis for Umu Agbai-Obete

The Total PAH concentration, as shown in **Figure 6(a)**, revealed distinct spatial variations in contamination levels across the Umu Agbai-Obete Axis. High PAH was observed at OYB 31 (Okpontu Township) and OYB 33 (Marihun Township), suggesting strong influences from industrial discharges, petroleum contamination, and commercial activities (Creegan & Gillett, 2020). In contrast, lower PAH concentrations were recorded at OYB 28 (Ban-Lori Market) and OYB 32 (Azuagu Township), indicating lower contamination exposure. The colour interpretation revealed that red/maroon regions correspond to high PAH, while blue regions indicate lower PAH levels (Yunker & MacDonald, 2019). The neutral/white areas represent moderate levels, forming transitional zones between highly contaminated and less impacted areas. The hexbin overlay further reinforces these findings, where hexagonal bins with darker red intensities confirm measured high PAH levels in key industrial and commercial zones (Lima & Mata, 2021).

The C8 - C16 fraction of TAH, represented in **Figure 6(b)**, exhibited spatial variability across the Umu Agbai-Obete Axis, with elevated contamination levels in commercial and industrial locations (Ruan & Liu, 2020). Higher C8 - C16 concentrations were recorded at OYB 28 (Ban-Lori Market) and OYB 29 (Obete Township), likely due to petroleum-related contamination, vehicular emissions, and market activities (Creegan & Gillett, 2020). In contrast, lower concentrations were noted at OYB 31 (Okpontu Township) and OYB 34 (Azumini Township), implying natural dispersion or reduced contamination input. The colour-coded interpretation indicated that red/maroon regions correspond to higher

concentrations, while blue regions indicate areas of lower contamination (Yunker & MacDonald, 2019). The C8 - C16 fraction is more volatile and degrades faster than heavier hydrocarbons; however, its presence in high-traffic areas raises concerns about airborne and soil contamination risks (González & O'Brien, 2021).

The C17 - C24 fraction of TAH, depicted in **Figure 6(c)**, exhibited a more persistent environmental presence across the area. Higher concentrations were recorded at OYB 28 (Ban-Lori Market), OYB 29 (Obete Township), and OYB 31 (Okpontu Township), indicating long-term retention and reduced degradation of these hydrocarbons (Ruan & Liu, 2020). Meanwhile, lower concentrations were observed at OYB 30 (Umu Agbai Township), OYB 33 (Marihun Township), and OYB 34 (Azumini Township), reinforcing the role of natural attenuation and dispersion in these areas. The C25 - C40 fraction of TAH, as illustrated in **Figure 6(d)**,

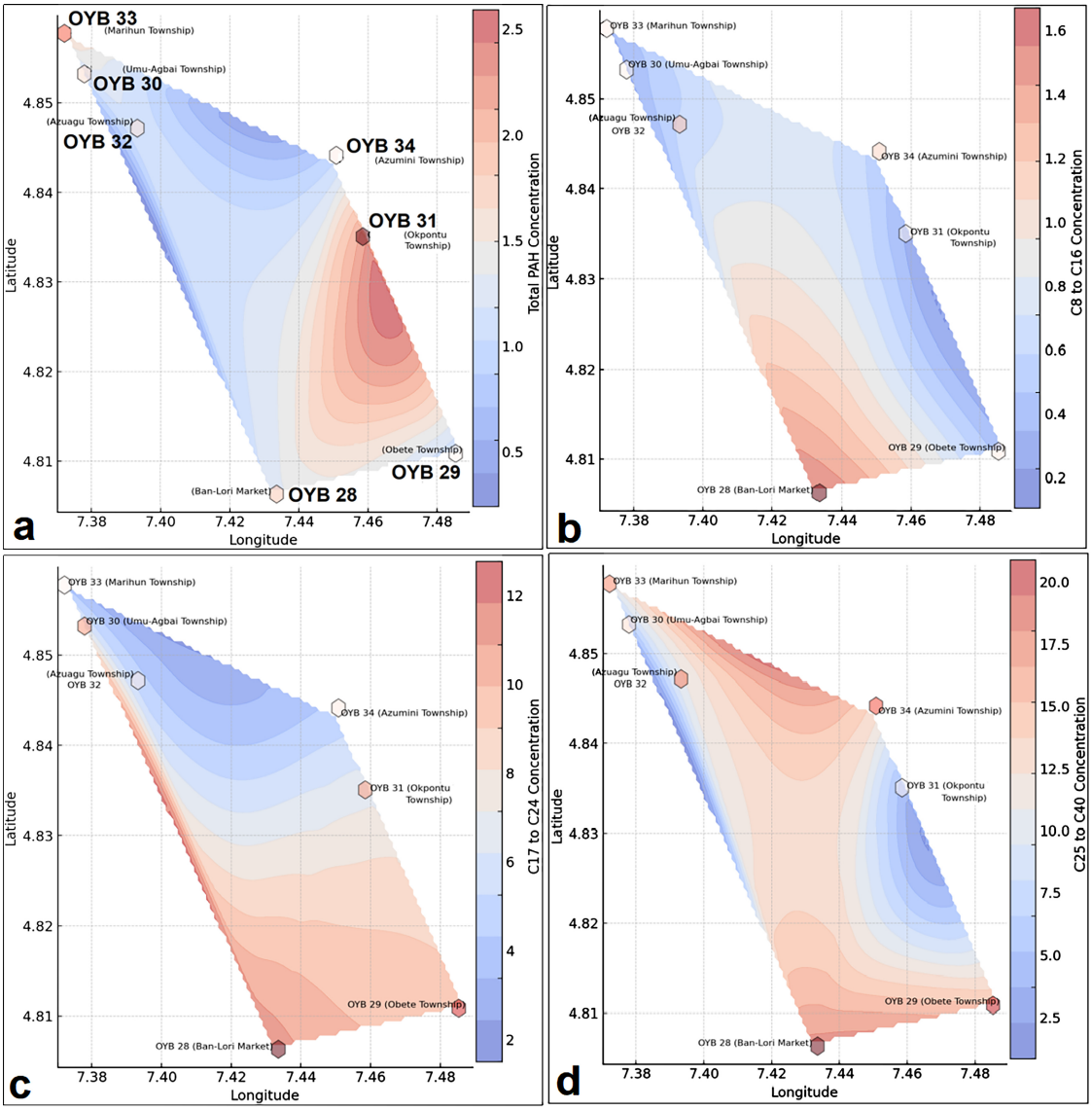

Figure 6. Dispersion for Umu Agbai-Obete. a) Total PAH, b) C8 to C16, c) C17 to C24, and d) C25 to C40 aliphatics.

demonstrated localized contamination patterns with limited mobility across the study area (Wang & Chen, 2020). Strong concentration zones were identified at OYB 28 (Ban-Lori Market), OYB 29 (Obete Township), and OYB 34 (Azumini Township), where petroleum residues and industrial emissions appeared to be the dominant contamination sources (Wang & Chen, 2020). Lower concentrations were observed at OYB 31 (Okpontu Township), OYB 30 (Umu Agbai Township), and OYB 33 (Marihun Township), suggesting reduced contamination exposure or enhanced degradation mechanisms. The color-coded spatial representation indicated that red/maroon regions corresponded to higher concentrations, while blue regions represented lower contamination levels (Lee & Park, 2021). The C25 - C40 hydrocarbons are highly persistent, tending to bind to soil and sediments, posing a long-term risk of environmental contamination that requires targeted soil and groundwater remediation strategies (Wang & Chen, 2020).

3.1.6. Integrated Hexbin and Contour Analysis of the Study Region

The plots in **Figure 7** represent the Hexbin density and spatial distribution of TPH concentrations across different sample stations. Warm colors (red, orange, yellow) indicate higher TPH concentrations, suggesting areas with significant contamination, whereas cool colors (blue, purple) indicate lower TPH levels (Nguyen & Tran, 2020). Gradient transition in contours helps identify hotspots of high contamination and diffusion trends, indicating potential hydrocarbon migration zones and natural attenuation zones where contamination is gradually reducing in regions with uneven TPH spread (Creegan & Gillett, 2020).

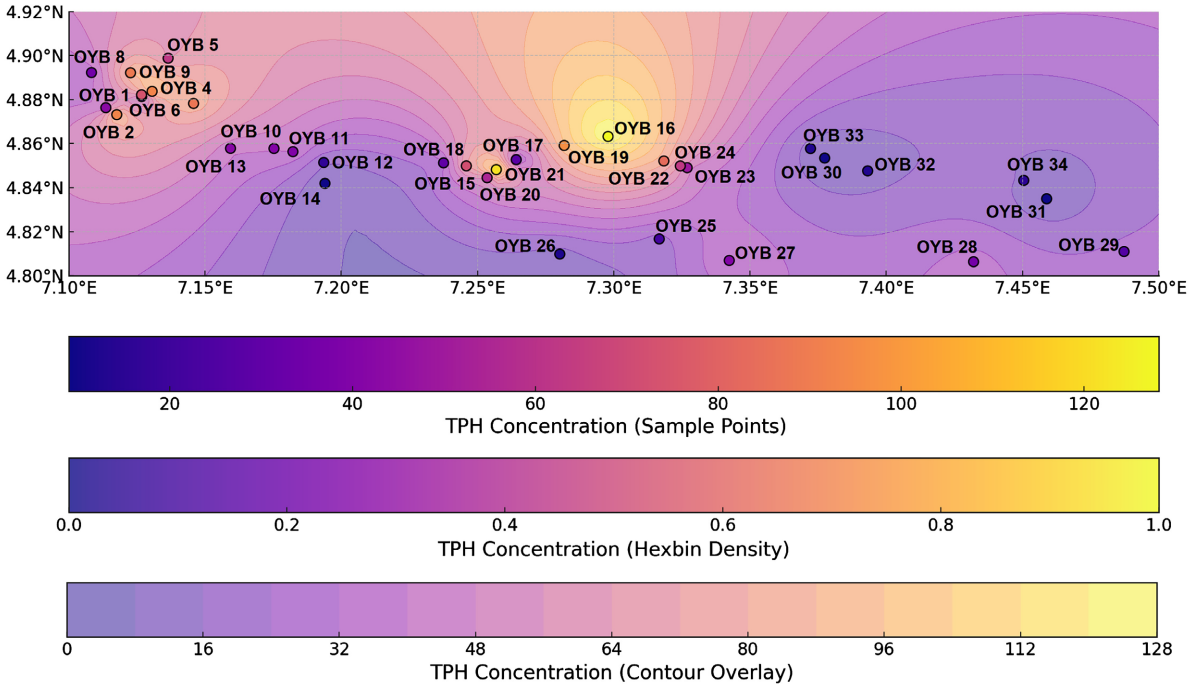

Figure 7. TPH dispersion across the study region.

Following the Hexbin density representation of the previously presented sub-regional locations, the study area was divided into hexagonal grids, where each hexagon represented the average TPH concentration within that localized region (Nguyen & Tran, 2020). The darker hexagons indicate higher contamination zones, while lighter hexagons indicate less contamination. This hexagonal density visualization helps identify contamination clusters, which could guide mitigation priorities and distinguish areas of local variability (Lee & Park, 2021). The Hexbin density comparison across the study area shows that the Western and Central locations and sample stations have dense dark hexagons, signifying persistent contamination, potentially from a continuous atmospheric medium of industrial and commercial petro-pollutants discharge (Nguyen & Tran, 2020). The Southern and Eastern sections, where lighter hexagons dominate, suggest lower contamination levels, possibly due to natural attenuation or dilution through atmospheric movement.

Contour overlay and spatial representation depict each black-circled point representing an actual sample station where TPH concentrations were measured. The colour of each point is directly linked to its measured TPH concentration, using the same scale as the contour and Hexbin map (Hwang & Kim, 2020). This allows for a direct comparison between actual measured values and interpolated estimations. Contaminant concentrations and characterization across the study area show that the Northern, Central, and North-Western sections, mainly Obigbo and Okoloma, exhibit higher TPH concentration patterns, as indicated by yellow/orange contours. This suggests long-term hydrocarbon impact from potential sources like vehicular exhaust, industrial discharge, or gas flaring activities (Lee & Park, 2021). The Eastern and South-Eastern sections, mainly Umu Agbai and Obete, represent locations of a gradual decrease in TPH levels (purple/blue transition), representing less contamination and suggesting dispersion of contaminants due to distance from source regions, atmospheric conditions, or proximity to natural pollution sinks like forests (Wang & Chen, 2020).

The integrated analysis and characterization show that the highest TPH concentrations are found in regions where red or orange contours overlap with dark hexagons, and sample stations indicate high values, reinforcing the accuracy of contamination hot zones. The potential migration zones are the areas with fewer sample points but steep concentration gradients, like regions where the contour colour changes abruptly. These suggest that petro-pollutant movement is occurring, likely due to wind flow or atmospheric moisture (Yunker & MacDonald, 2019). Lower TPH zones indicated by the blue or purple reflect areas less impacted by contamination, likely areas of atmospheric dilution, or natural processes mitigating the contamination levels.

3.2. Geochemical and Geospatial Correlation

Petro-pollutant atmospheric contamination, particularly through rainfall deposition, is a significant environmental concern in industrial and high-traffic regions (Lee & Park, 2021). The analyzed Total Petroleum Hydrocarbons (TPH),

including Total Aliphatic Hydrocarbons (TAH) and Total Polycyclic Aromatic Hydrocarbons (TPAH), serve as indicators of airborne pollution from fossil fuel combustion, transportation, gas flaring, and industrial emissions (Wang & Chen, 2020). The geochemical and geospatial correlation presents a comparative analysis of petro-pollutant fractions in rainwater samples collected across the five sub-regional locations (Obigbo, Komkom-Obiama, Okoloma, Egberu, and Umu Agbai-Obete) and thirty-four sample stations of the study region. This analysis evaluates the correlation between TPH, TAH, and TPAH across all study locations. It analyzes spatial variations in hydrocarbon pollutant deposition using latitude and longitude data and compares contamination trends between different locations to identify potential emission sources and high-risk zones. For all the locations (**Figures 8(a)-(e)**), the strong positive correlation (close to +1) between TPH and TAH indicates that aliphatic hydrocarbons are the dominant fraction of petroleum hydrocarbons in the independent location and sample stations.

Aliphatic hydrocarbons originate primarily from vehicular exhausts, industrial emissions, and fuel combustion, contributing significantly to atmospheric hydrocarbon pollution (Hwang & Kim, 2020). The dominance of TAH over TPAH suggests that a major source of airborne petroleum hydrocarbons in the different locations is fresh fuel combustion emissions rather than long-term industrial soot or heavy hydrocarbon residues (Yunker & MacDonald, 2019). Aliphatic hydrocarbons are more volatile and can be transported over long distances before being scavenged by rain (Schauer & Cass, 2019), explaining their widespread presence. This finding implies that air quality monitoring and emission control measures should focus on reducing transportation-related emissions, as they contribute significantly to hydrocarbon contamination in rainfall. The correlation matrix across the study region (**Figure 8(f)**) reveals consistent trends across the different locations. A strong positive correlation between TPH and TA H (>0.9) suggests that aliphatic hydrocarbons dominate petroleum hydrocarbon contamination in rainwater. In contrast, the moderate to weak correlation between TPH and TPAH indicates that PAHs originate from distinct sources and behave differently in the atmosphere (Lee & Park, 2021). The spatial correlations with latitude and longitude show regional variations in contamination trends and present the comparative deductions concerning the source, transport mechanisms and the pollutants' fate, reaffirming that higher pollution levels are concentrated in western and Northern locations (**Table 2**).

All locations exhibit a strong TPH-TAH correlation (>0.9), confirming that aliphatic hydrocarbons dominate hydrocarbon pollution across all locations. TPH-TPAH correlation varies between weak to moderate (~0.2 - 0.4), indicating diverse PAH sources, including gas flaring and biomass combustion (Feng & Zhang, 2021). Higher PAH levels in Okoloma and Umu Agbai-Obete suggest greater contributions from gas flaring and incomplete combustion processes (Hwang & Kim, 2020).

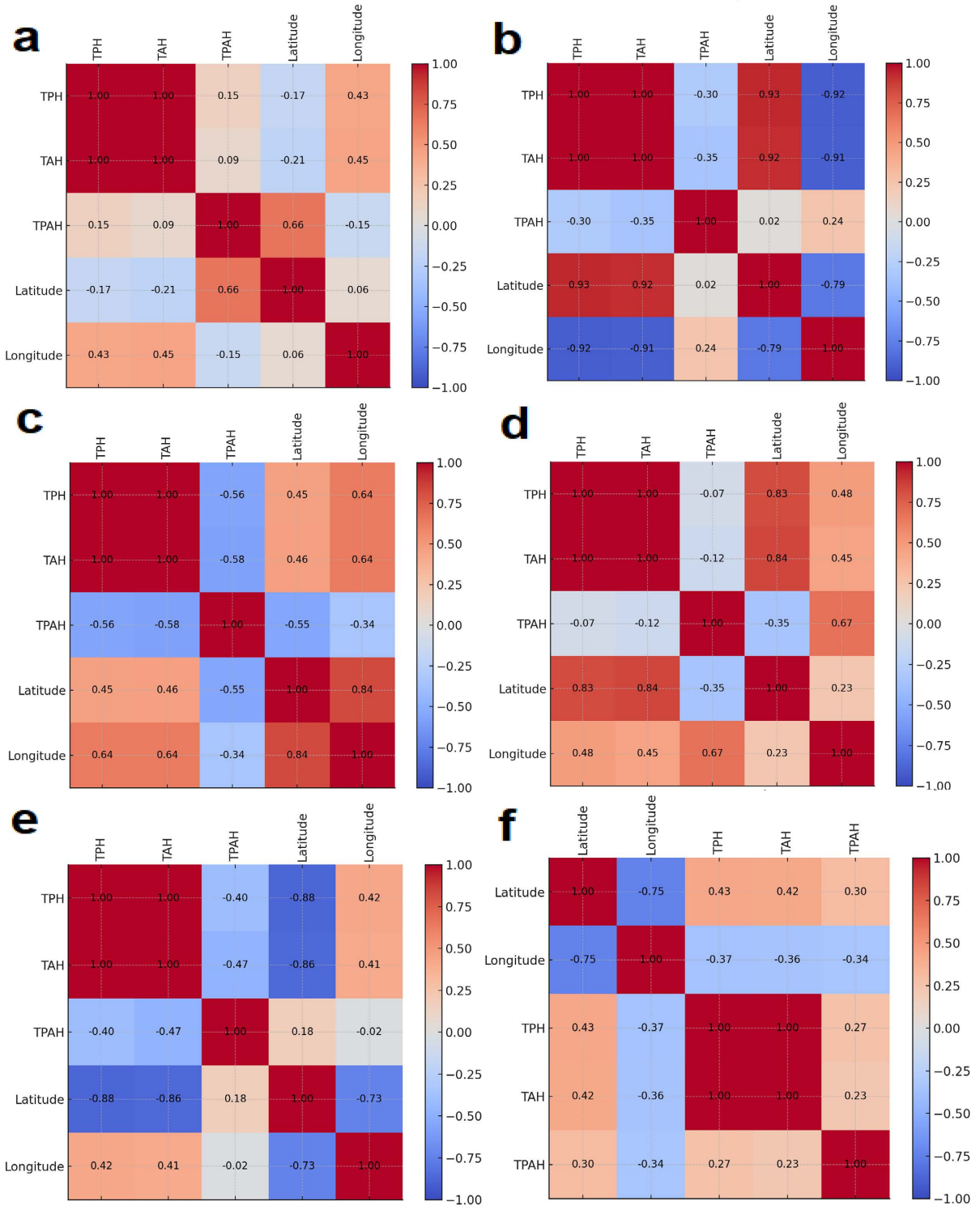

Figure 8. Correlation Matrix. a) Obigbo, b) Komkom-Obiama, c) Okoloma, d) Egberu, e) Umu Agbai-Obete, and f) Across the Study Region.

Hydrocarbon deposition trends by Latitude and Longitude provide further insights into spatial hydrocarbon deposition patterns across the study locations. For Longitude vs. TPH/TAH, the negative correlation in most locations suggests that

hydrocarbon contamination is higher in the Western and Northern parts of the study area. This trend is strongest in Obigbo and Komkom-Obiama, indicating primary pollution sources in these regions. Latitude vs. TPH/TAH presents a positive correlation in most locations, indicating higher hydrocarbon concentrations in the Northern region. Okoloma and Egberu show the strongest positive correlation, suggesting potential long-range transport of pollutants. These findings emphasize that local and regional emission sources contribute to hydrocarbon pollution, with Western and Northern locations experiencing the highest levels.

PAHs in rainwater pose carcinogenic and mutagenic risks, especially in communities relying on rainfall for water supply (Hwang & Kim, 2020). Inhalation of airborne hydrocarbons from rainfall-contaminated surfaces can contribute to respiratory diseases and chronic health conditions (Nguyen & Tran, 2020). Since the TPH-TAH correlation is highest across all locations, transportation emissions remain a primary contributor to hydrocarbon pollution. The higher PAH levels in Okoloma and Obigbo suggest a need for stricter enforcement of industrial emission standards and gas flaring regulations. There is a need for comprehensive air monitoring programs to track hydrocarbon pollution trends and implement evidence-based mitigation strategies.

Table 2. Regional correlation analysis and comparative deductions.

Location	TPH-TAH Correlation	TPH-TPAH Correlation	Key Findings	Source of Petro-Pollutants	Transport Mechanism	Fate of Pollutants
Obigbo	Strong (>0.95)	Weak to Moderate (~0.3)	High vehicular emissions and industrial activities drive TAH dominance.	Predominantly vehicular emissions and industrial discharges.	Atmospheric dispersion leading to deposition on water bodies.	Potential infiltration into soil and groundwater; volatilization into the atmosphere.
Komkom-Obiama	Strong (>0.92)	Weak (~0.2)	Lower PAH influence; likely dominated by fresh fuel combustion.	Fresh fuel combustion from local activities, possibly including small-scale refining.	Localized atmospheric transport with limited dispersion.	Rapid atmospheric degradation; minimal soil and water contamination due to low persistence.
Okoloma	Strong (>0.96)	Moderate (~0.4)	Higher PAH levels indicate contributions from gas flaring.	Gas flaring activities releasing unburnt hydrocarbons.	Emission of pollutants into the atmosphere with subsequent deposition.	Persistence in the environment due to the stable nature of PAHs; accumulation in soil and potential runoff into water bodies.
Egberu	Strong (>0.94)	Weak (~0.3)	Consistent with urban-industrial influence on aliphatics.	Urban-industrial activities, including machinery operations and transportation.	Atmospheric transport with deposition influenced by meteorological conditions.	Degradation varies; lighter aliphatics may volatilize, while heavier compounds can adsorb to soil particles.
Umu Agbai-Obete	Strong (>0.91)	Moderate (~0.4)	Mixed sources, including transport emissions and biomass burning.	Combination of vehicular emissions, industrial activities, biomass burning, and domestic fuel.	Complex transport pathways of atmospheric deposition and dispersion.	Diverse fate depending on compound; some may degrade rapidly, while others persist, leading to potential bioaccumulation.

4. Conclusion

This study provides an integrated hydrochemical dispersion and geospatial correlation analysis of aerial petro-pollutants in the Niger Delta, Nigeria, with a focus on hydrocarbon deposition through atmospheric pathways. The findings reveal that petroleum exploration, gas flaring, refining activities, and vehicular emissions significantly contribute to the accumulation of total petroleum hydrocarbons (TPH) in rainwater systems across the study region. Through compositional profiling of aliphatic hydrocarbons (C8 - C40) and polycyclic aromatic hydrocarbons (PAHs) using gas chromatography (GC-FID), this study identified aliphatic hydrocarbons as the dominant fraction, with strong correlations between TPH and total aliphatic hydrocarbons (TAH) ($r > 0.9$), indicating transportation-related emissions as the primary source. Localized PAH concentration spikes in industrial and gas-flaring zones further underscore the influence of fossil fuel combustion and petroleum-based industrial activities on hydrocarbon pollution.

The dispersion analysis, utilizing Hexbin and Contour mapping techniques, effectively visualized pollution hotspots and regional variations in hydrocarbon deposition. The results show that Western and Northern locations (particularly Obigbo and Okoloma) exhibit the highest hydrocarbon deposition, suggesting long-range pollutant transport and atmospheric dispersion effects. These contamination trends highlight the need for sustained environmental monitoring, stricter emission regulations, and targeted policies to mitigate the risks associated with petroleum-derived airborne pollutants in the Niger Delta. Given the widespread impact of hydrocarbon contamination on water resources, ecosystem health, and human exposure risks, this study underscores the urgency for enhanced air and water quality regulations, improved industrial waste management, and enforcement of gas flaring policies.

Based on the study findings, the following targeted recommendations are suggested: Stricter Regulatory Enforcement through implementing tighter controls on gas flaring and industrial emissions to reduce hydrocarbon pollution; Urban Planning Strategies through introducing buffer zones around high-risk industrial areas to minimize direct human exposure to airborne pollutants; Community-Based Monitoring Programs by establishing localized monitoring initiatives that engage local stakeholders in pollution tracking; Improved Waste Management Systems via the development of policies for cleaner fuel alternatives and proper disposal of petroleum residues to mitigate secondary contamination; and Green Infrastructure Solutions via implementing of phytoremediation techniques using hydrocarbon-degrading plant species in affected zones.

Future research should focus on seasonal hydrocarbon monitoring, detailed PAH speciation, and advanced atmospheric dispersion modeling to improve pollution source apportionment and inform sustainable environmental management strategies. By integrating hydrochemical assessments, spatial mapping, and multivariate statistical analysis, this research contributes to a more comprehensive understanding of petroleum hydrocarbon pollution dynamics in petroleum-pro-

ducing regions and provides valuable data for policymakers, environmental scientists, and regulatory bodies.

Acknowledgements

Profound gratitude is extended to Petrous Eco Geosolutions, Nigeria, for providing support for this study.

Author Contributions

Nurudeen Ahmed Onomhoale: Conceptualization, methodology, investigation, writing-original draft preparation, supervision, and resources. Luqman Jibril Yunusa: Writing-review and editing, and validation. Samson Senbore: Writing-review and editing, and validation. Dolapo Moses Apata: Writing-review and editing, and validation. Percy Ojogbo: Writing-review and editing, and validation. Emmanuel Samson Itiveh: Investigation, supervision, writing-review and editing, and validation.

Conflicts of Interest

The authors declare no conflicts of interest regarding the publication of this paper.

References

Ahmed, N. O., Daud, N. N. N., & Okunlola, I. A. (2024a). An Investigation of the Environmental Quality through Anthropogenic Metal Analysis in Targeted Niger Delta Aquatic Systems, Nigeria. In *Geography, Earth Science and Environment: Research Highlights Vol. 2* (pp. 91-115). BP International. https://doi.org/10.9734/bpi/geserh/v2/3212

Ahmed, N. O., Obafemi, A. A., & Udom, G. J. (2024b). Geospatial Variability and Distribution of Total Petroleum Hydrocarbons (TPH) in Soot-Contaminated Rain and Rivers at Oyigbo, Niger Delta, Nigeria. *Journal of Geography, Environment and Earth Science International, 28,* 1-30. https://doi.org/10.9734/jgeesi/2024/v28i3753

Ahmed, N. O., Suleiman, M. B., Olali, F. D., Ogunkoya, M. M., Oluwatobi, F. O., & Nwuzor, D. I. E. (2024c). Ionic Geospatialization and Hydrochemical Characterization of Water Resources around Selected Petroleum Producing Areas in South-Southern Nigeria. *Journal of Applied Geospatial Information, 8,* 19-40. https://doi.org/10.30871/jagi.v8i1.7406

Ahmed, N. O., Udom, G. J., & Obafemi, A. A. (2024d). Chemophysical and Metallic Characterization of Surface Water and Precipitation for Environmental Quality Assessment in Oyigbo L.G.A., Rivers State, Nigeria. *Journal of Global Ecology and Environment, 20,* 28-57. https://doi.org/10.56557/jogee/2024/v20i18562

Alao, B. M., Ateba, J. F. B., Gondji, D. S., Sabouang, J. F., Shouop, C. J. G., Ema'a, J. M. E., & Ben-Bolie, G. H. (2024). Assessment of Contamination Levels, Potential Ecological and Human Health Risks Due to Trace Elements Pollution in the Vicinity of the Lolodorf Uranium Deposit, Southern Cameroon. *Environmental Monitoring and Assessment, 196,* Article No. 1147. https://doi.org/10.1007/s10661-024-13218-5

American Institute for Conservation of Historic and Artistic Works (AICHAW) (2010). *The Hidden Hazards of Fire Soot.* https://www.culturalheritage.org/docs/default-source/publications/periodicals/newsletter/2010-09-sept-aicnews.pdf

Antai, R. E., Osuji, L. C., Obafemi, A. A., & Onojake, M. C. (2018). Air Quality Changes

and Geospatial Dispersion Modeling in the Dry Season in Port Harcourt and Its Environs, Niger Delta, Nigeria. *International Journal of Environment, Agriculture and Biotechnology, 3,* 882-898. https://doi.org/10.22161/ijeab/3.3.24

Baker, A., & Sillanpää, M. (2017). Anthropogenic Disturbances Impact the Natural Water Quality of a River System. *Environmental Science and Pollution Research, 24,* 28176-28189. https://doi.org/10.1007/s11356-017-0387-2

Baker, L. A., & Cormier, S. M. (2017). Using Heavy Metal Correlation Matrices to Distinguish Natural and Anthropogenic Influences in Contaminated Urban Streams. *Environmental Pollution, 224,* 398-407. https://doi.org/10.1016/j.envpol.2017.02.019

Bebeteidoh, O. L., Kometa, S., Pazouki, K., & Norman, R. (2020). Sustained Impact of the Activities of Local Crude Oil Refiners on Their Host Communities in Nigeria. *Heliyon, 6,* e04000. https://doi.org/10.1016/j.heliyon.2020.e04000

Chen, C., & Zhang, D. (2020). Environmental Behavior of Heavy Hydrocarbons: Transport, Adsorption, and Remediation Strategies. *Science of the Total Environment, 743,* Article 140649. https://doi.org/10.1016/j.scitotenv.2020.140649

Chinedu, E., & Chukwuemeka, C. K. (2018). Oil Spillage and Heavy Metals Toxicity Risk in the Niger Delta, Nigeria. *Journal of Health and Pollution, 8,* CID: 180905. https://doi.org/10.5696/2156-9614-8.19.180905

Cohen, A. J., & Coyle, A. (2019). The Effects of Volatile Hydrocarbon Components on Air Quality and Ecological Health. *Environmental Science & Technology, 53,* 1947-1955.

Creegan, M., & Gillett, N. (2020). Sources and Concentrations of Polycyclic Aromatic Hydrocarbons in Urban Environments: A Study of Industrial and Commercial Contributions. *Science of the Total Environment, 712,* Article 136486.

Crump, D. R., & Smith, S. W. (2020). Mechanisms of Natural Attenuation of Polycyclic Aromatic Hydrocarbons in Contaminated Sites: A Review. *Environmental Pollution, 256,* 113479.

Dale, A. M., & Boulton, A. J. (2019). Identifying Contamination Pathways for Petroleum Hydrocarbons in Urban Environments: A Multifaceted Approach. *Environmental Pollution, 244,* 1105-1115.

Daniel, J. (2003). *Sampling: A Conceptual Introduction. Sampling Essentials for Social Research.* Sage Publications.

Eneji, I. S., & Ogban, F. E. (2020). Monitoring Hydrocarbon Contamination and Assessing the Vulnerability of Water Bodies in Oil-Producing Regions. *Environmental Monitoring and Assessment, 192,* Article 347.

Enotoriuwa, R. U., Nwachukwu, E. O., & Ugbebor, J. N. (2016). Assessment of Particulate Matter Concentration among Land Use Types in Obigbo and Environs in Rivers State, Nigeria. *International Journal of Civil Engineering and Technology, 7,* 252-261.

Fang, J., & Zhao, S. (2021). Advances in Remediation Technologies for Contaminated Soils and Sediments. *Environmental Technology & Innovations, 22,* Article 101430.

Fawole, O. G., Cai, X.-M., & MacKenzie, A. R. (2016). Gas Flaring and Resultant Air Pollution: A Review Focusing on Black Carbon. *Environmental Pollution, 216,* 182-197. https://doi.org/10.1016/j.envpol.2016.05.075

Feng, Y., & Zhang, H. (2021). Analysis of Polycyclic Aromatic Hydrocarbons in Urban Rainwater: Sources and Health Implications. *Environmental Science and Pollution Research, 28,* 123-132.

Frolova, M. S., & Guo, H. (2020). Techniques for Visualizing Environmental Contamination: Hexbin and Contour Analysis. *Environmental Pollution, 261,* Article 114193. https://doi.org/10.1016/j.envpol.2020.114193

George, S. D., Ahmed, N. O., Yunusa, L. J., Senbore, S., & Yomi-Agbajor, E. B. (2023). Ecological and Human Health Impacts of Oil Spill-Induced Heavy Metal Contamination in the Niger Delta Environment, Nigeria: Post-Remedial Assessment, Risks, and Mitigation Strategies. *International Journal of Ecology and Environmental Sciences, 5,* 24-42.

Ghosh, U., & Sinha, S. (2020). Fate of Heavy Hydrocarbons in Soils: Insights from Field Studies and Laboratory Experiments. *Soil Biology and Biochemistry, 142,* Article 107711. https://doi.org/10.1016/j.soilbio.2020.107711

González, A. B., & Aroca, L. (2021). Spatial Distribution and Risk Assessment of Polycyclic Aromatic Hydrocarbons in Urban Soils and Sediments. *Environmental Monitoring and Assessment, 193,* Article 792.

Häggblom, M. M., & Bossert, I. D. (2021). Bioremediation of Persistent Petroleum Hydrocarbons: Mechanisms and Field Applications. *Environmental Science and Technology, 55,* 14534-14546. https://doi.org/10.1021/acs.est.1c03467

Hengl, T., & Gould, M. (2002). Weight of Evidence Modeling for Predicting the Spatial Distribution of Pollutants: An Application to the Assessment of Groundwater Quality. *Environmental Modelling & Software, 17,* 671-683. https://doi.org/10.1016/S1364-8152(02)00029-6

Hodge, M. M., & Hoque, M. (2011). A Multivariate Approach to Assess the Relationship between Water Quality Parameters and Hydrocarbon Concentrations in Urban Environments. *Water Research, 45,* 1340-1351.

Hwang, H. M., & Kim, S. (2020). Carcinogenic Risks of Polycyclic Aromatic Hydrocarbons in Rainwater: A Review of Health Impacts. *Environmental Health Perspectives, 128,* Article 028001.

Hwang, H., & Park, B. (2021). Persistence and Degradation of Semi-Volatile Organic Compounds in Soil and Water: Implications for Environmental Monitoring. *Chemosphere, 263,* 128-137.

Inyang, S. E., Aliyu, A. B., & Oyewale, A. O. (2018). Total Petroleum Hydrocarbon Content in Surface Water and Sediment of Qua-Iboe River, Ibeno, Akwa-Ibom State, Nigeria. *Journal of Applied Sciences and Environmental Management, 22,* 1953-1959. https://doi.org/10.4314/jasem.v22i12.1

Kim, M., Hong, S. H., & Won, J. (2013). Petroleum Hydrocarbon Contaminations in the Intertidal Seawater after the Hebei Spirit Oil Spill: Effect of Tidal Cycle on the TPH Concentrations and the Chromatographic Characterization of Seawater Extracts. *Water Research, 47,* 758-768.

Koch, J., & Schneider, M. (2019). Hydrochemical Response of Groundwater to Land Use Changes in a Small Agricultural Watershed. *Hydrology and Earth System Sciences, 23,* 1253-1265.

Kumar, R., & Singh, K. P. (2018). A Study of Environmental Monitoring of Rainwater Quality in Urban and Rural Water Bodies in India. *Environmental Monitoring and Assessment, 190,* Article 112.

Lee, J., & Park, J. (2021). Visualization Techniques for Spatial Analysis of Environmental Contaminants: A Case Study Using Hexbin and Contour Analysis. *Journal of Environmental Management, 284,* Article 112035.

Li, Z., & Wong, D. W. S. (2018). Spatial Analysis of Environmental Pollutants: A Comparative Study between Hexagonal and Rectangular Grids. *Environmental Modelling & Software, 104,* 103-112.

Lima, A. P., & Mata, A. M. (2021). Persistent Environmental Contaminants: An Overview of Pristane and Phytane in Natural Ecosystems. *Environmental Science & Technology, 55,* 10325-10336. https://doi.org/10.1021/acs.est.1c01234

Liu, H., & Liu, S. (2020). Spatial Analysis of Environmental Contaminants Using Hexbin and Contour Interpolation Methods. *Applied Geography, 111,* 102-110.

Liu, Y., & Wang, Y. (2019). Correlation Analysis among Hydrocarbon Fractions and Water Quality Indicators in Petroleum-Contaminated Groundwater. *Journal of Environmental Management, 243,* 255-263. https://doi.org/10.1016/j.jenvman.2019.05.012

Luan, W., & Szelewski, M. (2008). Ultra-Fast Total Petroleum Hydrocarbons (TPH) Analysis with Agilent Low Thermal Mass (LTM) GC and Simultaneous Dual-Tower Injection. In *Agilent Technologies Application Note: Environmental* (pp. 1-8). Agilent Technologies, Inc. https://www.agilent.com/cs/library/applications/5990-3201EN.pdf

Manisalidis, I., Stavropoulou, E., Stavropoulos, A., & Bezirtzoglou, E. (2020). Environmental and Health Impacts of Air Pollution: A Review. *Frontiers in Public Health, 8,* Article 14. https://doi.org/10.3389/fpubh.2020.00014

Mason, O. U., & Brubaker, K. L. (2019). The Role of Urban Landscapes in the Distribution of Polycyclic Aromatic Hydrocarbons in Soil and Water. *Environmental Pollution, 246,* 546-556. https://doi.org/10.1016/j.envpol.2018.12.046

Mohamed, E. S., Jalhoum, M. E. M., Hendawy, E., El-Adly, A. M., Nawar, S., Rebouh, N. Y. et al. (2024). Geospatial Evaluation and Bio-Remediation of Heavy Metal-Contaminated Soils in Arid Zones. *Frontiers in Environmental Science, 12,* Article 1381409. https://doi.org/10.3389/fenvs.2024.1381409

Moore, G. K., Roberts, I. A., & Kelly, E. J. (2023). Spatial Analysis of Hydrocarbon Contamination in Urban Settings: Impacts, Patterns, and Implications for Land Management. *Environmental Monitoring and Assessment, 195,* 102-115.

Müller, H. J., & Meyer, J. (2021). Geospatial Data Analysis and Visualization with Python: A Framework for Effective Environmental Monitoring. *Environmental Science & Technology, 55,* 3480-3490.

Nadim, F., & Hossain, K. (2021). Polycyclic Aromatic Hydrocarbons (PAHs) in the Environment: Sources, Exposure, and Risk Assessment. *Environmental Toxicology and Chemistry, 40,* 2767-2790.

National Bureau of Statistics (2006). *Social Statistics Report*. National Bureau of Statistics Nigeria.

Nguyen, H. T., & Tran, T. H. (2020). Assessing Contamination Hotspots in Urban Areas Using Hexbin Visualization Methods. *Environmental Monitoring and Assessment, 192,* Article 259.

Obenade, M., Ekwugha, E. U., Okeke, H. U., & Okpiliya, I. F. (2020). An Assessment of the Environmental Impacts of Land Use Dynamics in Eleme, Rivers State, Nigeria. *IOSR Journal of Environmental Science, Toxicology and Food Technology, 14,* 41-55.

Ojelede, M. O., & Kafadar, A. (2023). Hydrochemical Monitoring and Spatial Pollution Analysis in the Niger Delta: Implications for *S*Environmental Management.*cience of the Total Environment, 868,* Article 161523.

Okorhi-Damisa, F. B., Ogunkeyede, A. O., Akpejeluh, P., & Okechukwu, L. (2020). Analysis of Soot in Rainwaters around Warri Metropolis. *International Journal of Scientific Development and Research, 5,* 319-325.

Omokpariola, D. O., Nduka, J. K., Kelle, H. I., Mgbemena, N. M., & Iduseri, E. O. (2022). Chemometrics, Health Risk Assessment and Probable Sources of Soluble Total Petroleum Hydrocarbons in Atmospheric Rainwater, Rivers State, Nigeria. *Scientific Reports, 12,* Article No. 11829. https://doi.org/10.1038/s41598-022-15677-7

Onwuka, C., Eboatu, A. N., Ajiwe, V. I. E., & Morah, E. J. (2021). Pollution Studies on Soils from Crude Oil Producing Areas of Rivers State, Niger Delta Region, Nigeria. *Open Ac-*

cess Library, 8, 1-17. https://doi.org/10.4236/oalib.1107583

Opu-Ogulaya, E. D. W. (1973). *History of the Creation of the Rivers State of Nigeria: Primer One*. Government Printer.

Rapaport, R. A., & Guers, L. R. (2019). Volatility Characteristics of Hydrocarbon Fractions and Implications for Ambient Air Quality. *Atmospheric Environment, 200,* 118-126.

Ruan, X., & Liu, Y. (2020). Volatility, Dispersion, and Environmental Fate of Light Hydrocarbons in Urban Environments. *Environmental Research Letters, 15,* Article 105005.

Sadiq, R., & Al-Sharif, A. (2020). Environmental Monitoring and Evaluation Techniques for Sustainable Water Resource Management in Oil-Contaminated Areas. *Resources, Conservation and Recycling, 150,* Article 104445.

Samuel, P., Elechi, O., & Julius, N. E. (2022). Total Hydrocarbon Contents: Spatial Variations in Aquatic Environment of Oyigbo Communities, Rivers State. *International Journal of Environmental Protection and Policy, 10,* 1-5.

Schauer, J. J., & Cass, G. R. (2019). Volatile Organic Compounds and Atmospheric Transport: A Study of Hydrocarbon Emissions from Motor Vehicles. *Environmental Science & Technology, 53,* 4690-4699.

Schwarzenbach, R. P., Gschwend, P. M., & Imboden, D. M. (2005). *Environmental Organic Chemistry* (2nd ed.). Wiley.

Siciliano, S. D., & Enkiri, N. K. (2019). Environmental Risks Associated with Adsorption of Hydrocarbons in Soil. *Environmental Pollution, 252,* 802-810.

Teixeira, C. J., & Nearing, M. A. (2019). Soil and Water Sampling: Principles and Application. *Agricultural Water Management, 221,* 469-476. https://doi.org/10.1016/j.agwat.2019.05.014

United Nations Environment Programme (UNEP) (2021). *Emerging Issues in Water and Health: Policy Perspectives from the UN Environment Assembly*. United Nations Environment Programme.

Wang, R., & Chen, L. (2020). Heavy Hydrocarbons in Soil: Mobility, Persistence, and Contamination Risks. *Science of the Total Environment, 740,* Article 140051.

Yunker, M. B., & MacDonald, R. W. (2019). The Role of Spatial Variability in Heavy Metal and PAH Contaminants: Insights and Implications for Environmental Monitoring. *Environmental Pollution, 254,* Article 113144.

Zhang, T., & Zhang, Y. (2019). Mechanisms of the Chemical Degradation of Petroleum Hydrocarbons in the Environment: Insights and Applications to Bioremediation. *Environmental Science & Technology, 53,* 8839-8847.

Zhou, J., Wang, C., Chen, J., & Wu, Y. (2020). Health Risk Assessment and Sources of Polycyclic Aromatic Hydrocarbons in a Typical Oil-Producing Area: A Case Study in China. *Environmental Science and Pollution Research, 27,* 41558-41568.